Synthetic Modification and HAPs Generation Activity of Environmental Benign Citrate, Gallate/Chitosan Intercalated Mg Al-Layered Double Hydroxides (LDHs) for Biomedical Engineering Applications

[1,2]Sehar Zahid, [1,2]Waqas Jamil, [3]Mouhammad Taha, [2]Javeria Shaikh and [4]Khalid Mohammad Khan
[1]*Dr. M.A. Kazi Institute of Chemistry, University of Sindh, Jamshoro.*
[2]*Institute of Advanced Research Studies in Chemical Sciences, University of Sindh, Jamshoro.*
[3]*Department of Clinical Pharmacy, Institute for Research and Medical Consultations (IRMC), Imam Abdulrahman Bin Faisal University, Dammam, Saudi Arabia.*
[4]*H. E. J. Research Institute of Chemistry, International Center for Chemical and Biological Sciences, University of Karachi, Karachi-75270, Pakistan.*
waqas.jamil@usindh.edu.pk*

(Received on 12 December 2023, accepted in revised form 23rd August 2024)

Summary: Nowadays, biocompatible, and cost-effective material design is one of interesting fields in biological process. In this regard, Magnesium/Aluminum Layered Double Hydroxides (Mg/Al LDHs) synthesized and fabricated with environmental benign anions was investigated like Citrate and Gallate. Furthermore, these modified Mg/Al LDHs were treated with chitosan in order to increase the biocompatibility of the compounds. The Fourier-Transform Infrared (FTIR), Scanning Electron Microscopy (SEM), Energy dispersive X-ray (EDX) and X-ray Diffraction (XRD) analysis confirmed that modification has done successfully. In FTIR the peaks appeared in the range of 3441 cm^{-1} to 3380 cm^{-1} were attributed as acidic OH^- . Whereas, the metal oxide peaks appeared below 1000 cm^{-1} showing the successfully intrusion of anions. Moreover, the plate like structure in SEM analysis also confirmed the successful modification of anions. The presence of elemental peaks through EDX including: Ca, P, N as well as Mg, Al and the gap between these layers calculated through XRD endorsed the intercalation of anions in LDHs. The thermal stability profile revealed that the thermal stability of modified Mg/Al LDHs has decreased than pure Mg/Al LDHs due to incorporation of organic segments. These synthetically modified Mg/Al LDHs were evaluated for their Hydroxyapatites [Ca_{10} $(OH)_2$ $(PO_4)_6$] generation ability in Simulated Body Fluid (SBF) at pH 7.4. The results showed that the modified Mg/Al LDHs have significant Hydroxyapatites (HAPs) generation ability. Moreover, the citrate intercalated LDH showed remarkable bioactivity in term of HAPs generation. Therefore, these modified Mg/Al LDHs have excellent capability to utilize these compounds in various fields like: bone and teeth additives, implant materials as well as bone- tissue engineering.

Keywords: Modified Mg/Al/Hydroxide, Environmental Benign, Simulated Body Fluid, Hydroxyapatites

Introduction

Biotechnology has drawn the attention of the world due to its multiple applications, particularly in the field of medicine where it promotes the productivity of medicinal proteins and different drugs. Whereas, in the meantime, Nano-structured materials are also playing a phenomenal role along with various remarkable applications in tissue, biological, as well as surface engineering etc [1-3].

Currently, Nano composite (NC) compounds are widely being synthesized with proficient thermal and mechanical performance which is based on polymeric matrices and has been evaluated in modern industries. A number of nano composites have been reported for their mechanical strength, toughness and electrical or thermal conductivity [4-5]. Layered Double Hydroxides (LDHs) are delineated by the general formula [M^{2+1}-x Mx $^{3+(}$OH)2] Ax/n-n.mH^2O, have two-dimensional anionic clays structure, whereas the cationic metals possess the charges of two and three respectively, moreover, anionic charges retained between the LDH layer is shown by the symbol Ax [6]. The negative interlayer anion charges neutralized the positive charges in this layer [7].

In recent times, intercalation of LDH with various organic molecules is catching the attention of researchers in current research for various applications and development, like: sensing materials [8], water treatment [9], and for drug delivery [10].

Citric Acid (CA) and Gallic Acid (GA) are the organic compounds present in citrus fruits and pineapple. Citric Acid (CA) is an aliphatic compound with one hydroxyl and three carboxyl acid groups in its structure as showing in Fig 1(a), while Gallic Acid (GA) is an aromatic molecule that has three hydroxyl and one carboxyl acid groups as given in Fig 1(b). CA intercalated Al Zn- LDH and carbon dots treated

*To whom all correspondence should be addressed.

CA modified Al-Zn Nano composite has been found for its astonishing results to enhanced thermal stability and high optical clarity of PVA and improvement of RO membranes respectively [11-12]. Whereas, Gallic acid modified Layered Double Hydroxides (LDHs) has been reported with controlled release and antioxidant activity [13]. Chitosan (CS) is a peculiar compound that is used vastly for the preparation of artificial bio-nano composites [14-16] Chitosan is usually a non-hazardous, inexpensive, bio-compatible, and eco-friendly compound [17]. Its specialty is that it has a wide surface area, high temperature sustainability and excellent anionic exchange response. Therefore, it can be applied in various fields, like drug delivery, fuel cell, water purification, biosensors, in medical and so on [18-19]. The un-branched bio-compatible molecules having hydroxyl and amine functional groups react and intermingle with the other molecules and enhance their properties [20]. Therefore, CS NCs having LDH Nano-layers are exceptionally attractive due to lightweight, biodegradable, and environmentally benign performance. CS/LDHs have been investigated for insulin electrical signal, reparation of bone constituents and preparation of superlative oxygen barrier films [21-22].

The study of regeneration of the human skeleton by various biocompatible materials that are damaged by traumas, injuries, infections, or gerontic changes with deprivation of bone mass as well as volume is one of the attractive fields in medical science [23-24].

The biocompatible substitute materials by the regenerative mechanism improving mechanical strength through the backup function of the skeleton and rejuvenating the current tissue viable because of their compatible nature [25-26]. Therefore, the modern materials are superficially bioactive and exposed macro porosity to provide the required area for angiogenesis and augmentation of bone tissue. In the literature, there are numerous materials that are used for hard tissue engineering, such as bioactive glasses, [27-32] and polymer composites with metal (Ti, Zr) alloys etc. [33-38]. Though all of these modified bio-compatible compounds have various advantages in drug delivery system, tissue engineering and biomedical applications, but do not fulfill the complete requirement of fully intermingle and efficient therapeutic solution. The Hydroxyapatite (HAPs) [Ca_{10} $(OH)_2PO_4)_6$], is more likely to be inorganic materials, likewise, teeth, bones and other mammalian tissues [39-40]. HAPs have a crystal structure and highly thermally stable compound [41-42]. HAPs materials have various applications in the medical field due to their remarkable Osteo-conductive behavior as well as exceptional biocompatibility and bioactivity [43]. Hence, the current proclivity of researchers is the proliferation of hydroxyapatite (HAPs) on the surface of NCs material with enhanced properties.

Thus, herein we are reporting the synthesis and evaluation of two bio-compatible modified nano composites i.e. Al-Mg citrate/chitosan and Al-Mg gallate/chitosan LDHs for the production of HAPs in Simulated Body Fluid (SBF).

In this regard, we have designed to synthesize these molecules due to their structural features and bio-compatibility.

Materials and Methods

Materials

All the chemicals [Al $(NO_3)_3.9H_2O$] and [Mg $(NO_3)_2.6H_2O$], Na–Citrate, Na-Gallate, NaOH, Acetic acid and, Chitosan were purchased from Sigma-Aldrich.

Procedure for the Synthesis of Mg/Al - LDH

The compound was synthesized according to literature [6]. A mixture of Mg $(NO_3)_2 \cdot 6H_2O$] and [Al $(NO_3)_3 \cdot 9H_2O$] with a molar ratio of 3:1 dissolved in 50ml deionized water. The mixture was stirred along with the addition of sodium hydroxide (2M) drop wise till pH 10 was achieved. The solution becomes milky white and that solution was refluxed for 16h. After filtration, the obtained compound was washed with distilled water until pH -7, and then these precipitates were dried in an oven at 80 ℃ for 10 h and marked as Mg/Al LDH.

Method for the Modification Mg/Al-LDH with Citrate/ Gallate

A mixture of Mg/Al-LDH was refluxed with Na- Citrate and Na-Gallate separately for 10h in dist. water. Afterwards, the white and brown color precipitates for citrate and gallate ion intercalated LDHs were obtained respectively. These solutions were filtered, washed with dist. water and dried at 65℃ and marked as Citrate modified Mg/Al- LDH and Gallate modified Mg/Al -LDH.

Procedure for the Proliferation of Citrate /Gallate Modified Mg Al – LDH with Chitosan (CS)

The above synthesized Citrate and Gallate modified Mg/Al-LDHs were further treated with Chitosan. For that purpose, 2g chitosan dissolved in 1% AcOH, stirred for 5 min and a transparent solution was obtained. Meanwhile, in a separate Round Bottom(RB) flask added 4g of Citrate modified Mg/AL-LDH mixed with 2ml chitosan solution and another RB flask added 4g of Gallate modified Mg/AL-LDH mixed with 2ml chitosan solution and stirred the mixtures for 6h. After due time, the precipitates were filtered off, washed with dist. water, and dried and marked as Citrate modified- LDH/ Chitosan and Gallate modified-LDH/ Chitosan NCs.

Preparation of Simulated Body Fluids (SBF)

The Simulated Body Fluid prepared according to the reported method [44]. The compounds consist of NaCl (8.03 g), KCl (0.225 g), 1.0M HCl (39.0 ml), $CaCl_2$ (0.292 g), $MgCl_2{\cdot}6H_2O$ (0.311 g), $NaHCO_3$ (0.355 g), $K_2HPO_4{\cdot}3H_2O$ (0.231 g), Na_2SO_4 (0.072 g), and $(HOCH_2)_3CNH_2$ were mixed in 1000 ml of deionized water and 1.0M HCl added drop wise as par requirement to maintain pH = 7.4 The bottle was shaken gently and stored in refrigerator for further process. Simultaneously, the pH of solution was monitored according to the erstwhile study [45].

Procedure for Haps Generation by Modified LDHs in SBF

Citrate/gallate/chitosan modified Mg/Al–LDH nano composites with different amounts i.e 0.3g and 0.6g were soaked into 30 ml SBF at room temperature for 30 days and kept unshaken. The pH of all four solutions was monitored during reaction time. After 30 days, Citrate modified Mg Al-LDH/CS and Gallate modified Mg Al-LDH/CS NCs layers were separated out and subjected to SEM and EDX analysis.

Results and Discussion

Preparation of Citrate modified Mg Al -LDH / CS and Gallate modified Mg Al- LDH/CS Nano Composites and their Implication of Intercalation

In this current research work, the Citrate and Gallate molecules which were intercalated into Mg Al-LDH layers to form a CA modified Mg Al LDH and GA modified Mg Al LDH. . These molecules have characteristic structural feature like Citric Acid (CA) Fig 1 (a) is an aliphatic structure with one –OH and three carboxylic acid groups while Gallic Acid (GA) Fig 1 (b) is aromatic in nature with three –OH and one carboxylic group. Whereas the further modification with chitosan is also beneficial due to its eco-friendly, and biodegradable nature. The above molecules used for the modification of Mg/Al LDH has already been reported for their biological potential as well as environmental benign in nature [45, 46].

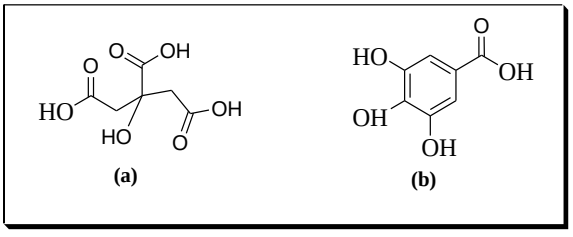

Fig. 1: Structures of (a) Citric acid (b) Gallic acid.

In addition, the polar groups present in CA and GA molecule can participate in escalation of functional groups in the structure of LDH compounds. The Fig 2 represents the schematic structure of Citrate and Gallate intrusion into LDH which further explain the interaction of H-bonding in LDH layers with the intercalated Citrate and Gallate molecules. Moreover, there can be seen a slight electrostatic collaboration within the positive charges of LDHs and the negative charges of Citrate and Gallate molecules. Although the treatment of these two modified LDHs with the CS explains the enhancement of surface area with the interaction with the H-bonding of LDH layers as well as elevated bio-compatibility.

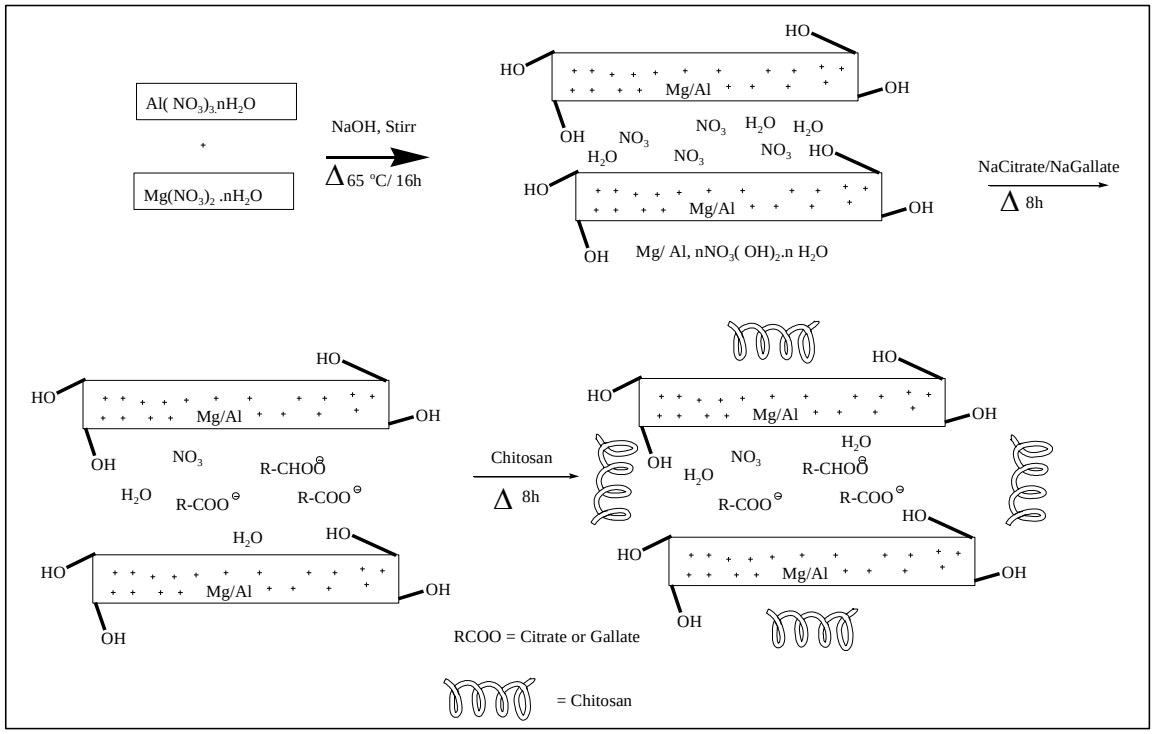

Fig. 2: Synthetic Scheme for Citrate/Gallate modified Mg-Al LDH/Chitosan.

Characterization Techniques

FTIR Spectral Analysis of Citrate/Gallate modified Mg Al - LDH/Chitosan

The modified and fabricated samples were analyzed *via* Fourier-Transform Infrared Spectroscopy (FTIR). In Fig 3 exhibits the FTIR results for (**a**) Pure Mg Al-LDH (**b**) Citrate modified Mg Al-LDH (**c**) Citrate modified Mg Al –LDH/ CS (**d**) Gallate modified Mg Al-LDH (**e**) Gallate Modified Mg Al-LDH / CS. For (**a**) peak appeared at 3441 cm^{-1} was assigned for –OH starching vibration due to interlayer –OH or H_2O molecule. The absorption band at 1384 cm^{-1} was assigned for $–NO_3$ group. A weak band at 1648 cm^{-1} was due to bending modes of H_2O molecules. The peaks at 810 cm^{-1} and 741 cm^{-1} associated with M-O-H vibrations. (**b**) The broader and intense absorption band at around 3450 cm^{-1} was due the hydrogen bonded network of layered –OH and water molecules. The peak appeared at 1583 cm^{-1} designated for carbonyl group and the peaks in the range of 1392 cm^{-1} - 1020 cm^{-1} were due to the replacement of nitrate groups with some guest anions as stretching vibration of COO^- citrate anions. Moreover, the weaker band at around 2370 cm^{-1} was owing to the aliphatic C-H stretching. The peak observed in (**c**) at about 3490 cm^{-1} was attributed to the –OH stretching. The peaks observed in the range 1100 cm^{-1}-1400 were due the presence of Carbon, Nitrogen and oxygen present in chitosan. The band at the position at 1591 cm^{-1} and 1172 cm^{-1} were due to C=O and C-O-C stretching respectively. The peaks revealed in the range 1480 cm^{-1}- 1592 cm^{-1}were assigned to primary amine N-H and C-H stretching as well. Besides this, (**d**) the band appeared at 3380 cm^{-1} exhibited the presence of acidic -OH stretching. The C-H stretching in gallic acid was assigned at the position in the range 2110 cm^{-1} -2440 cm^{-1}. The band appeared at 1672 cm^{-1} was due to the intercalated carboxylate group. Also, the peak found at 1385 cm^{-1} was allotted as nitrate group as co-intercalated and absorbs species. Moreover, the C-H bending vibration of benzene ring was assigned at 1392 cm^{-1}. In addition to that, (**e**), the peaks with a hump analyzed at around 3500 cm-1 indicated the OH stretching with amine group in chitosan. Adding more, the CH_2 stretching was observed at 2972 cm^{-1}, Including the peak at 1594 cm^{-1} assigned as the C=O stretching in chitosan molecule-H bending was also witnessed at the assigned position 1641 cm^{-1}.

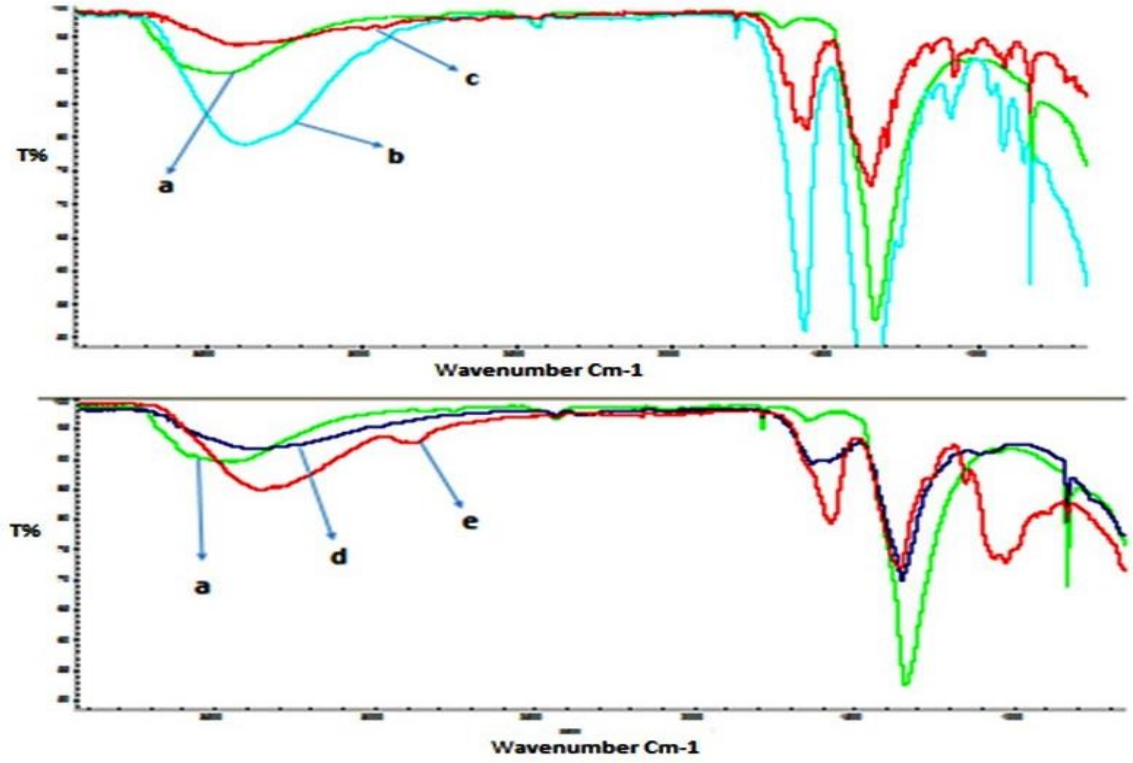

Fig 3: FT-IR of (a) Pure Mg-Al LDH (b) Citrate modified Mg Al-LDH (c) Citrate modified –Mg Al-LDH/ CS (d) Gallate modified Mg Al-LDH (e) Gallate modified Mg Al -LDH/ CS NCs .

XRD Analysis

The XRD analysis was used to notice the crystal structure of the provided samples through Bragg's Law [Eq. (1)] which was applied for the calculation of basal spacing (d) of LDH layers:

$$n\lambda = 2d\sin\theta \qquad (1)$$

Where n = reflection coefficient and is equal to 1

λ = wavelength and it is akin to 1.51418 Å
θ = Bragg- Brentano geometry

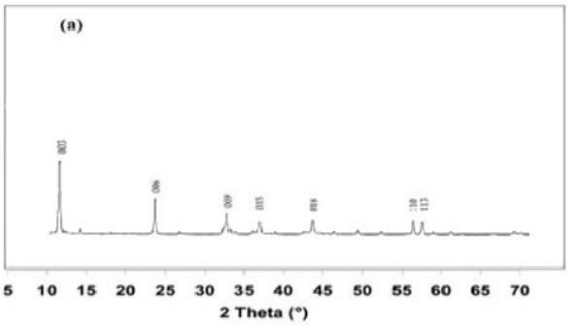

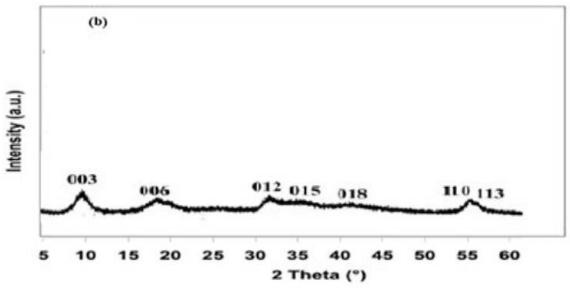

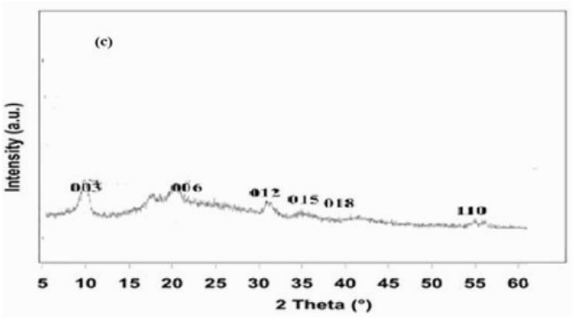

Fig. 4: The XRD pattern of (a) pure Mg Al-LDH (b) Citrate modified Mg Al-LDH/CS (c) Gallate modified Mg Al-LDH/CS.

Table-1: 2θ Interlayer space values (a) Pure MgAl –LDH (b) Citrate modified MgAl -LDH/CS (c) Gallate modified MgAl-LDH/CS.

S. No	Peak Intensity	Interlayer space d-Spacing (nm) (a)	Interlayer space d-Spacing (nm) (b)	Interlayer space d-Spacing (nm) (c)
1	003	7.37	8.91	8.83
2	006	3.86	4.92	4.23
3	012	2.71	2.79	2.71
4	015	2.43	2.56	2.49

The XRD analysis for Pure Mg Al- LDH (**a**) at 2θ equivalent to 7.37, 3.86, 2.71, 2.43 according to peak intensity at (003), (006) and (012),(015) respectively. The d-spacing values of (**b**) Citrate modified Mg Al-LDH/ Chitosan and (**c**) Gallate modified Mg Al- LDH/ Chitosan at the positions (003), (006), (012), (015) were calculated by the formula given in equation (**1**).The d-spacing values were found to be 8.91, 4.92, 2.79, 2.56 for Citrate modified Mg Al-LDH/ Chitosan and 8.83, 4.23, 2.71, 2.49 Gallate modified Mg Al- LDH/ Chitosan Fig. 4 (a,b,c). Comparatively, 2θ values of Citrate and Gallate modified Mg Al- LDH/ Chitosan were shifted from lower to high 2θ values than the pure Mg Al-LDH, which is a clear indication of the intrusion of large size anions and broadened the space amid the layers consequently.

SEM and EDX Analyses

The Surface study and elemental composition of the compounds were evaluated by Scanning Electron Microscope (SEM) and Energy Dispersive X-Ray analysis (EDX) respectively. **Fig 5** shows the topography of (**a**) pure Mg Al-LDH (**b**) Citrate modified Mg Al-LDH (**c**) Citrate modified Mg Al-LDH/ CS (**d**) Gallate modified Mg Al-LDH (**e**) Gallate modified Mg Al-LDH/CS with the visible morphological changes with increasing the surface area of such thread like chitosan surrounded the surface of modified LDH.

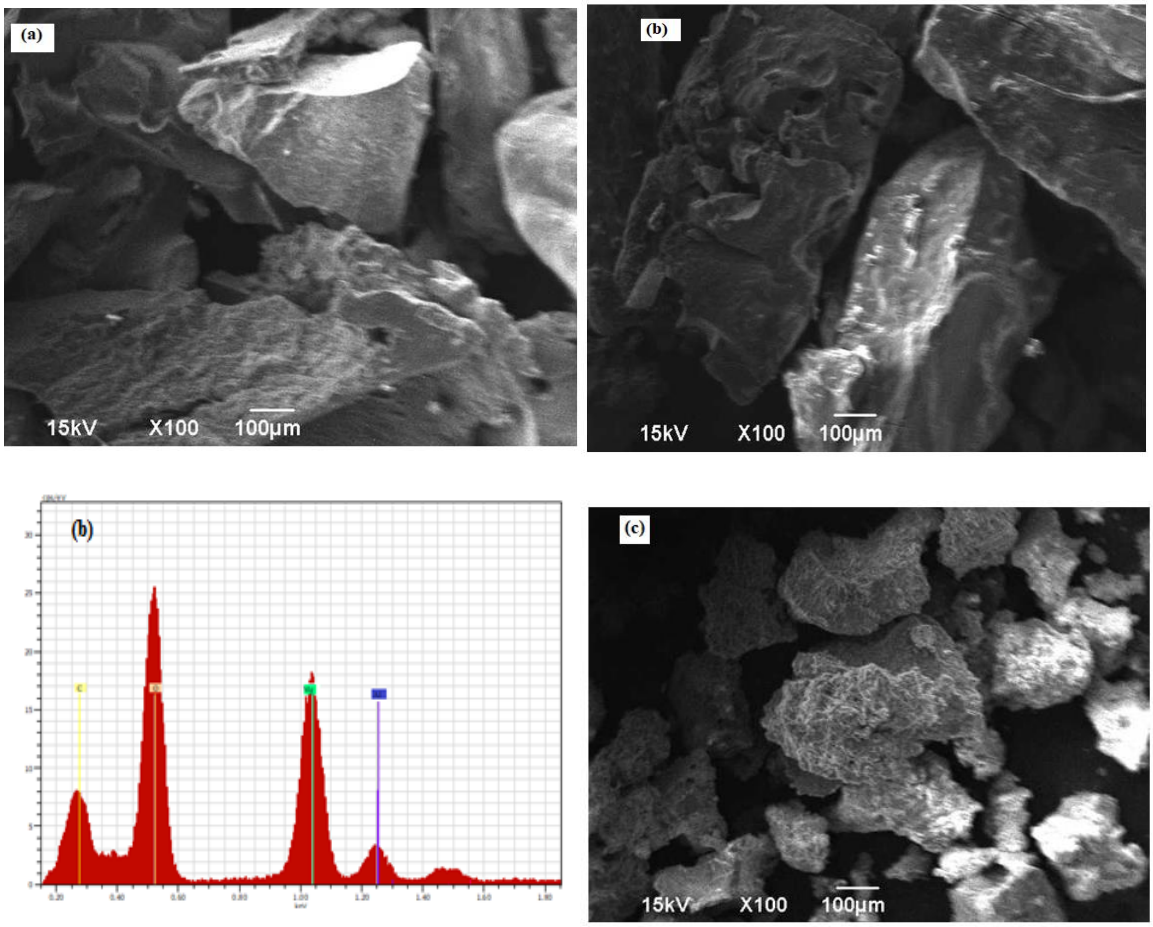

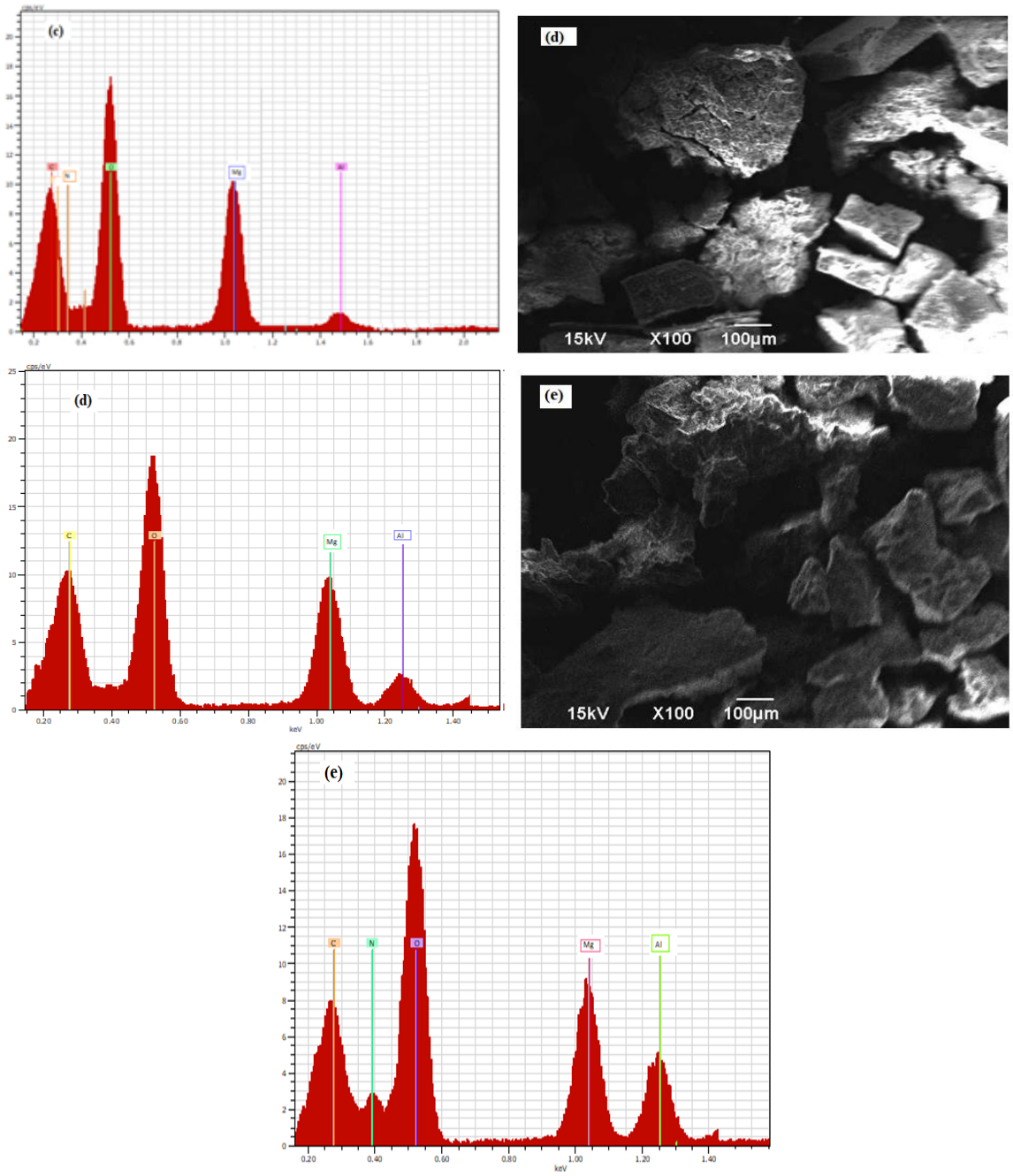

Fig. 5: SEM &EDX (a) Mg Al -LDH (b) Citrate modified Mg Al-LDH (c) Citrate modified Mg Al-LDH/ CS (d) Gallate modified Mg Al-LDH (e) Gallate modified Mg Al-LDH/CS.

Here, the SEM images Fig 5 (a) showing the plate like structure of pure Mg Al-LDH. The comparison of morphology with pure Mg Al–LDH, confirms the effect of guest ions intervention as well as the extended surface ratify the besiege of LDH through CS molecules. The topographic changes were observed after the intercalation of Citrate and Gallate anions Fig 5 (b,d). Furthermore, upon treatment with chitosan, it was perceived in Fig 5 (c, **e**) that the polymeric chains encapsulated the LDHs. The thread like overlapping can be seen in SEM images of the Citrate and Gallate modified Mg Al-LDH/CS nano composites with the increased surface area. These results were also confirmed by FTIR described earlier.

Thermogravimetric Analysis

The thermal decomposition profile of synthesized LDH shown in Fig 6(a). According to TGA curve of LDH there are three main steps: the first step occurs between 40 ℃ to 170 ℃ with mass loss of 8%. This event corresponds to dehydration of weakly bounded surface as well as interlayer space water molecules. The second step started from 235 ℃ and end up to 336 ℃. The 8% mass loss observed in this step is related to the putrefaction of the hydroxide layers. The third step (480-780 ℃) with 50% mass loss might be due to decomposition of - NO_3 anions from the inter lamellar space leading to the collapse of the layered structure concomitantly with the oxide crystallization [47].

TGA curve of Mg/Al/citrate/CS and Mg/Al/gallate/CS Fig 6 (b, c) also presents events that can be divided into three main steps. The first event started from 40℃ to 218 ℃ (mass loss of 14%) and it is related to the dehydration process. The second step is observed from 218 ℃ to 480 ℃ (mass loss of 31%) and it is assigned to the occurrence of concomitant events: (i) the release of water molecules from dehydroxylation process of the LDH layers; (ii) the decomposition of the adsorbed and intercalated citrate or gallate anions. The third step occurs at temperatures above 580 ℃ and the small weight loss of CO_2 can be associated from intercalated anions as shown in Fig 6 (c). According to thermogravimetry pattern, the modified LDHs have more volatile products than pure LDHs, supporting the proposal of citrate/gallate/chitosan adsorption/intercalation into the inorganic adsorbent.

HAPs Generation Bioactivity

In the perspective of the judgment of kokubo, the compounds that have the ability to form the bone like Hydroxyapatite (HAP) materials are known as bioactive compounds [48, 49]. The HAPs $[Ca_{10}(OH)_2(PO_4)_6]$, generation bioactivity can be measured in Simulated Body Fluid (SBF). The SBF composition is same as human blood plasma. Here, following the same perception the Citrate modified Mg Al-LDH/CS and Gallate modified Mg Al- LDH/ CS were soaked separately into the SBF solution to investigate the formation of HAPs on the surface of synthesized LDHs. In this regard, the measured amount (0.3 and 0.6) of Citrate modified Mg Al-LDH/CS and Gallate modified Mg Al- LDH/ CS immersed in SBF for 30 days Fig7 (a, b). The initial pH was observed 7.4.

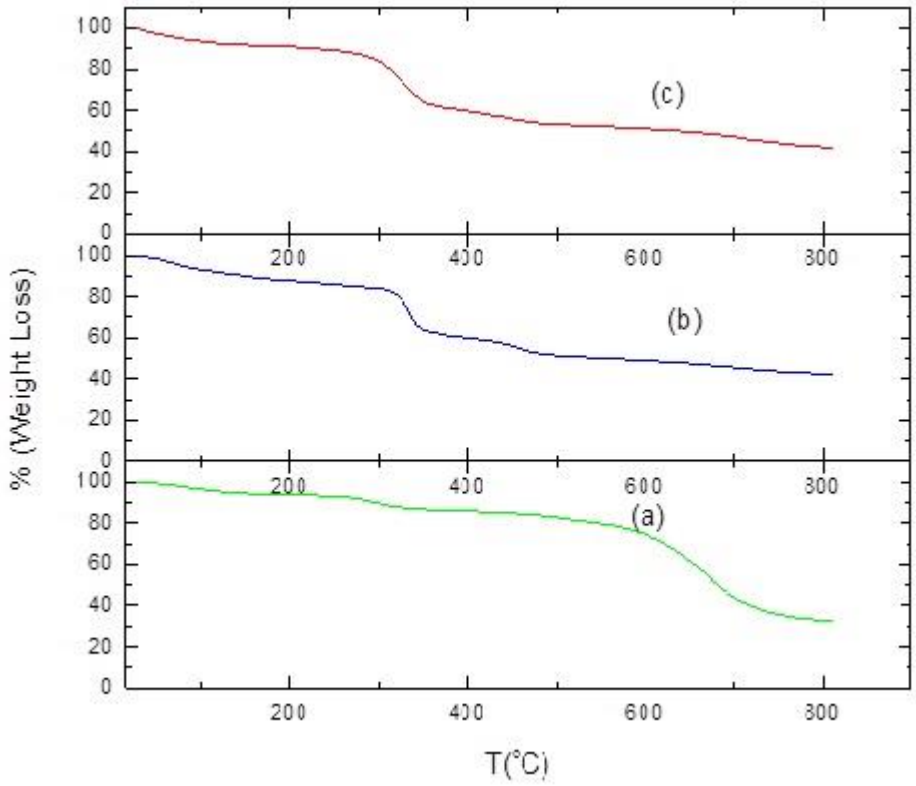

Fig. 6: Thermograms of (a) Mg/Al LDH (b) Mg/Al/Citrate/CS (c) Mg/Al/Gallate/CS.

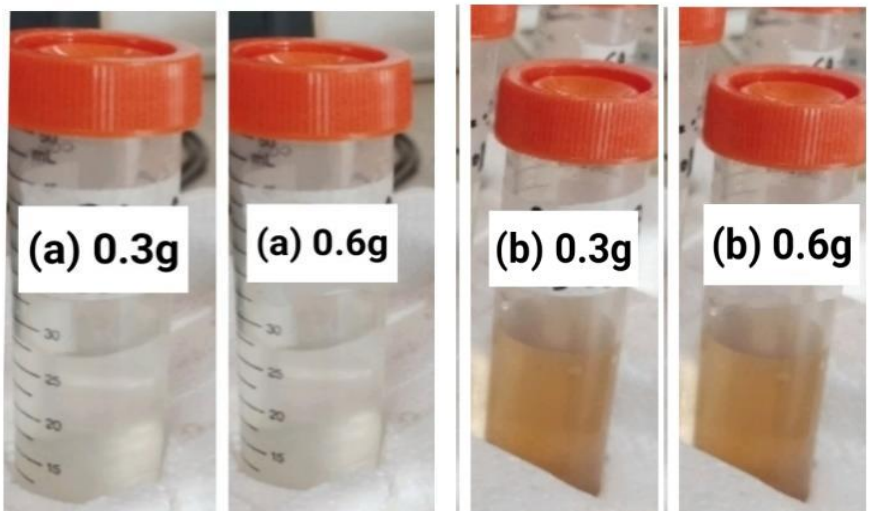

Fig. 7: (a) Citrate modified Mg Al- LDH/CS (b) Gallate modified Mg Al- LDH/ CS.

Since, day-1 to day-7, there was no significant changes observed in pH for Citrate/Gallate modified Mg Al-LDH//CS, although, with the passage of time from day-8 to day-20, pH was increased up to 8.5, whereas, the decline of pH from. 8.5 to 7.3 were detected from day 21 to day-30 Fig 8 (a,b).The reason for surging pH to high value can be due to the adsorption of H^+ in the SBF solution through the LDHs, which added the positive charges on the surface. Subsequently, LDHs with the high positive charge surface have the ability to adsorb phosphate ion taken from SBF [51]. During this time a steady growth of layers were observed on the surface of LDHs which is taken as sign of generation of HAPs. These layers were separated out after 30 days and inculcated pH results well in the samples containing 0.6 g of modified LDHs and subjected to SEM/EDX analysis for the study of morphological changes during the process.

Relatively, the visible morphological changes were observed in SEM images of Citrate modified Mg Al-LDH/CS and Gallate modified Mg Al-LDH/CS after 30 days immersion in SBF Fig 9 (a,b) than LDHs before immersion into SBF Fig 6 (c and e). These morphological variations are due to formation of HAPs on the surfaces of LDHs. When in fact, the comparison between the SEM images of Fig 9 (a) Citrate modified LDH/CS and (b) Gallate modified LDH/CS, it can be seen that the Citrate modified LDH/CS has the porous surface after the formation of HAPs on the surface, although no such prominent alteration was observed in Gallate modified LDH/CS.

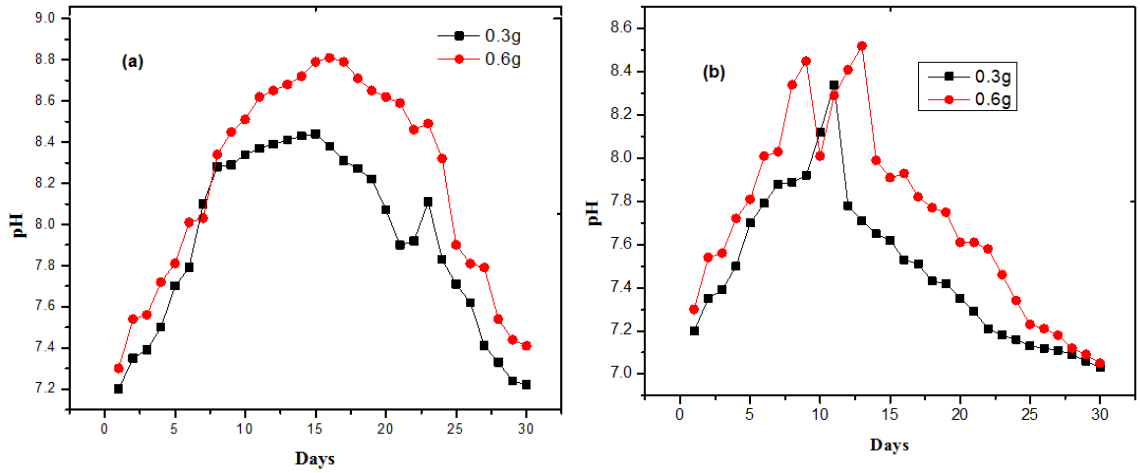

Fig. 8: pH Study of synthesized (a) Citrate modified Mg Al-LDH/CS (b) Gallate modified Mg Al-LDH/CS.

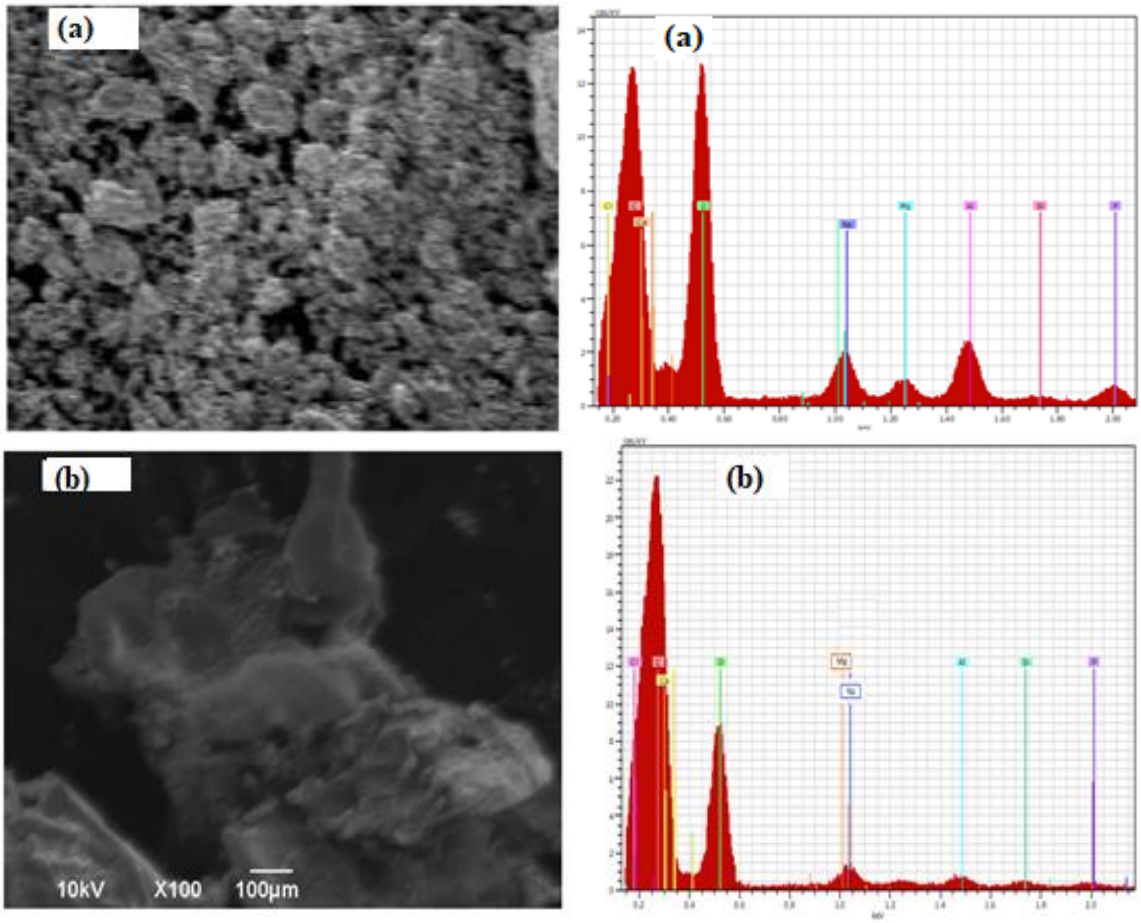

Fig. 9: SEM/EDX images (a) Citrate modified LDH/CS and (b) Gallate modified LDH/CS after 30 days in Simulated.

Body Fluid (SBF)

Though, bright particles were revealed on the surfaces of both LDHs after immersion for 30 days. These particles were due to HAPs formation. Furthermore, generations of HAPs were also established by EDX analysis. The Peaks for calcium and phosphorous in EDX confirmed that HAPs [$Ca_{10}(OH)_2(PO_4)_6$] are successfully generated on the surfaces of Citrate and Gallate modified LDH/CS.

Moreover, it was found that Citrate modified LDH/CS showed better activity in term of Haps formation, than Gallate modified Mg Al-LDH/CS. The high intensity peaks for Ca and P in EDX was observed in former LDH. Therefore, it is reflected that citrate modified LDH/CS have better ability to adsorb Ca and P than Gallate modified LDH/CS which has miscellaneous surface and lower adsorption of Ca and P on its surface.

The reason of development of HAPs on the surface of Layered Double Hydroxide (LDH) might be due to the -OH groups on the surface of LDHs layers that enhanced the functional groups of nano composites along with increment of interactions with the ions present in Simulated Body Fluid (SBF) and promulgate the growth of Haps in samples. Beside this, the de-protonation on the surface of Nano Composites (NC) and simultaneous adsorption of Ca on the negative surface which ultimately made the surface more positive. Secondly, the positive sites of NCs have the capability to adsorb (PO_3^{-4}) from the SBF and with replication of the process causes the formation of HAPs on the surface of Citrate/Gallate modified Mg Al- LDH/CS NC films.

Conclusion

It is concluded from the above-mentioned work that the CA and GA are the biological molecules with high potential that can be utilized in eco-friendly industry. In current study we have used

co-precipitation method for the intercalation of Citrate and Gallate ions with Layered Double Hydroxide (LDH) in basic condition. The guest ions Citrate and Gallate accommodated in nano LDH by increasing the interlayer distance for Citrate/Gallate modified LDH. The bioactivity of the modified LDHs were also observed by soaking Citrate/ Gallate modified LDH/CS NC films into SBF solution for 30 days, and witnessed the growth of HAPs on the surface of layer which were evidenced through SEM images. Apart from this the formation of HAPs on the surface was also verified through results of EDX and FT-IR as well. Hence, it is concluded that the bio-NCs of such type have the admirable capability to be utilized in various fields like: bone and teeth additives, implant materials as well as bone- tissue engineering.

Acknowledgement

The authors are highly thankful to Higher Education Commission (HEC) of Pakistan for their financial support for this project under the umbrella of Indigenous Ph.D. Fellowship for 5000 Scholars, HEC (Phase II).

References

1. S. Mallakpour, M. Hatami, Highly capable and cost-effective chitosan Nano composite films containing folic acid-functionalized layered double hydroxide and their in vitro bioactivity performance, *J. Mat. Chem and Phys*., **250**, 123044 (2020)
2. M. Majumdar, S. Shivalkar, A. Pal, M.L. Verma, A.K. Sahoo, D.N. Roy, Nanotechnology for enhanced bioactivity of bioactive compounds, in: M. Verma, A. Chandel (Eds.), *J. Biotech. Prod of Bio. Comp*., 433-466 (2020)
3. P. Ginestra, Manufacturing of poly caprolactone-graphene fibers for nerve tissue engineering, *J. Mech. Behav. Biomed. Mater*.,100 (2019)
4. N.H. Othman, M.C. Ismail, M. Mustapha, N. Sallih, K.E. Kee, R.A. Jaal. Graphene- based polymer nanocomposites as barrier coatings for corrosion protection, *J. Prog. Org. Coat*., **135**: 82 (2019)
5. X. Wu, S. Takeshita, K. Tadumi, W. Dong, S. Horiuchi, H. Niino, T. Furuya, S. Yoda, Preparation of noble metal/polymer nanocomposites via in situ polymerization and metal complex reduction, *J. Mat. Chem. and Phys*., **222,** 300 (2019).
6. N. Rasouli, M. Movahedi, M. Doudi,, Synthesis and characterization of inorganic mixed metal oxide nanoparticles derived from Zn–Al layered double hydroxide and their antibacterial activity, *J. Surf and Interf* .,**6**, 110 (2017).
7. J. P. E Machado, R.A. de Freitas, F. Wypych, Layered clay minerals, synthetic layered double hydroxides and hydroxide salts applied as pickering emulsifiers, *J.Appl. Clay. Sci*..,**169**, 10 (2019).
8. A. Kausar, Versatile epoxy/polyaniline and derived nanocomposite: from strategic design to advance application, *J. Mat. Res. Inn*., **25**, 321 (2021).
9. Q. Fang, S. Yang, H., Yang, K., Zhou, J., Gao, Y., Lin, Q. Tan.Z, Application of layered double hydroxide-biochar composites in wastewater treatment: Recent trends, modification strategies and outlook *J. Haz. Mat*., **420**, 126569 (2021).
10. B. Xue, H.Zhang,L.Dou, Layered Double Hydroxide-Based Nanocarriers for Drug Delivery, *J. Phar*.,**6**, 298 (2014).
11. M. Dinari, A.Nabiyan, Citric acid-modified layered double hydroxides as a green reinforcing agent for improving thermal and mechanical properties of poly(vinyl alcohol)-based nanocomposite films, *J. Poly. Comp*., **38**, 128 (2017).
12. L. W. Liang, J. M Gao, Z. H. Huang, H. Zhang, M. P. Li, X. Zhang, X. H. Ma, and Z.L. Xu, Layered double hydroxide modified polyamide reverse osmosis membrane for improved permeability, *J. Des .Wat. Tre*., **203**, 35 (2020).
13. M Silion, D.Hritcu, G.Lisa, M.I. Popa, New hybrid materials based on layered double hydroxides and antioxidant compounds. Preparation, characterization and release kinetic studies, *J. Por. Mat.*, **19**, 267 (2012).
14. P. Beulah, U. Jinu, M.Ghorbanpour, P.Venkatachalam, Green engineered chitosan nanoparticles and its biomedical applications-An overview, *J.Adv .Phyt.*, 329-341 (2019).
15. P. Zhao, Y. Zhao, L. Xiao, H. Deng, Y. Du, Y. Chen, X. Shi, Electrodeposition to construct free-standing chitosan/layered double hydroxides hydro-membrane for electrically triggered protein release, *J. Col and Surf B: Biointer*., **158**, 474 (2017).
16. J. Yuan, S. Xu, H.-Y. Zeng, X. Cao, A. Dan Pan, G.-F. Xiao, P.-X. Ding, Hydrogen peroxide biosensor based on chitosan/2D layered double hydroxide composite for the determination of H_2O_2, *J.Bio. electr.chem*., **123**, 94 (2018).

17. A. Chatterjee, P. Bharadiya, D. Hansora, Layered double hydroxide based bio nano composites, *J. Appl. Clay.Sci*., **177**, 19 (2019).
18. N. Chubar, R. Gilmour, V. Gerda, M. Micusík, M. Omastova, K. Heister, P. Man, J. Fraissard, V. Zaitsev, Layered double hydroxides as the next generation inorganic anion exchangers: synthetic methods versus applicapability. *J.Adv. Col and Inter. Sci.*, **245**, 62 (2017).
19. E. Seftel, R. Ciocarlan, B. Michielsen, V. Meynen, S. Mullens, P. Cool, Insights into phosphate adsorption behavior on structurally modified ZnAl layered double hydroxides, *J.Appl. Clay. Sci*., **165**: 234 (2018).
20. L. Mao, H.Q. Wu, Y.J. Liu, J. Yao, Y.K. Bai, Enhanced mechanical and gas barrier properties of poly(ε-caprolactone) nanocomposites filled with tannic acid-Fe(III) functionalized high aspect ratio layered double hydroxides, *J. Mat. Chem and Phys*., **211**, 501 (2018).
21. Y. X. Chen, R. Zhu, Z.L. Xu, Q.F. Ke, C.Q. Zhang, Y.P. Guo, Self-assembly of pifithrin-α-loaded layered double hydroxide/chitosan nanohybrid composites as a drug delivery system for bone repair materials, *J.Mat. Chem B.*, **5**, 2245 (2017).
22. T. Pan, S. Xu, Y. Dou, X. Liu, Z. Li, J. Han, H. Yan, M. Wei, Remarkable oxygen barrier films based on a layered double hydroxide/chitosan hierarchical structure, *J.Mat. Chem. A.*,**3**, 12350 (2015).
23. E. Gyo˝ri, I. Fábián and I. Lázár, Effect of the Chemical Composition of Simulated Body Fluids on Aerogel-Based Bioactive Composites, *J. comp. sci*., **1,**15 (2017).
24. A. Luetke, P.A .Meyers, I.Lewis,H. Juergens, Osteosarcoma treatment where do we stand? A state-of-the-art review, *J.Can.tre.rev*., **40,** 523 (2014).
25. J. R. Jones, New trends in bioactive scaffolds: The importance of nanostructure, *J. Eur Cer Soci*., **29**, 1275 (2009).
26. C. K. Wei, & S. J. Ding, Acid-resistant calcium silicate-based composite implants with high-strength as load-bearing bone graft substitutes and fracture fixation devices, *J. Mech. Beh.Biomed.Mat*., **62,** 366 (2016).
27. J.Van der Stok, E.M.M.Van Lieshout,Y.El-Massoudi, G.H. Van Kralingen, P.Patka, Bone substitutes in the Netherlands—A systematic literature review, *J. Acta. biomate* **7**,739 (2011).
28. A. Abdal-hay, A. S.Hamdy, K. A.Khalil, J. H. A. Lim, A novel simple in situ biomimetic and simultaneous deposition of bone like apatite within biopolymer matrix as bone graft substitutes, *J.Mat.Lett*.,**137**, 260 (2014).
29. C. Liu, P. Wan, L. LTan,.K. Wang, K. Yang, Preclinical investigation of an innovative magnesium-based bone graft substitute for potential orthopaedic applications, *J.Ortho.Trans*., **2**, 139 (2014).
30. J. Tusnim, M. E Hoque, Bio resorbable bone graft substitutes. In Bone Substitute Biomaterials, *J.Biomed. Engi. Else*.,113 (2021).
31. J. Lacroix, E. Jallot, J. Lao, Gelatin-bioactive glass composites scaffolds with controlled macroporosity, *J.Chem. engi*, **256**, 9 (2014).
32. E. Vernè, S. Ferraris, C.Vitale-Brovarone, A. Cochis,L. Rimondini, Bioactive glass functionalizd with alkaline phosphatase stimulates bone extracellular matrix deposition and calcification invitro, *J.Appl .surf. Sci*., **313**, 372 (2014).
33. I. Mutlu, Sinter-coating method for the production of Tin-coated titanium foam for biomedical implant applications, *J.Surf and Coat. Tech*., **232**, 396 (2013).
34. J. Rivard, V. Brailovski, S. Dubinskiy, S. Prokoshkin, Fabrication, morphology and mechanical properties of Ti and metastable Ti-based alloy foams for biomedical applications, *J.Mat.Sci.EngiC*., **45**, 421 (2014).
35. E. Butev, Z.Esen, S. Bor, bioactivity investigation of alkali treated Ti6Al7 N alloy foams, *J.Appl. Surf. Sci* .**327**, 437 (2015).
36. E. Fidancevska, G. Ruseska, J. Bossert, Y. M. Lin,. A. R. Boccaccini, Fabrication and characterization of porous bioceramic composites based on hydroxyapatite and titania, *J.Mat. Chem and Phys*., **103**, 95 (2007).
37. F. Miculescu, A. C. Mocanu, C. A. Dascălu, S. Maidaniuc, D. Batalu, A. Berbecaru, S. I. Voicu, M. Miculescu, V. K. Thakur, L. T. Ciocan,, Facile synthesis and characterization of hydroxyapatite particles for high value nanocomposites and biomaterials, *J. Vacu*., **146**, 614 (2017).
38. F. Miculescu, A. Maidaniuc, S. I. Voicu, V. K. Thakur, G. E.Stan, L. T.Ciocan, Progress in Hydroxyapatite–Starch Based Sustainable Biomaterials for Biomedical Bone Substitution Applications, *JACS. Sust. Chem. Engi*., **5**, 8491 (2017).
39. F. Castro and A. Ferreira, Characterization of intermediate stages in the precipitation of hydroxyapatite at 37 C, *J.Chem. Engi. Sci* .,**77**, 150 (2012).
40. H. A. Kim and B. K. Kim, Synthesis and properties of waterborne polyurethane/

hydroxyapatite chemical hybrids, *J. Prog. Org. Coat*., **128**, 69 (2019).

41. V. Saxena, I. Shukla, L. M. Pandey, Hydroxyapatite: an inorganic ceramic for biomedical applications, *J.Elsev*., 205 (2019).
42. A. Molaei, M. Yari, M.R. Afshar, Investigation of halloysite nanotube content on electrophoretic deposition (EPD) of chitosan-bioglass-hydroxyapatite-halloysite nanotube nanocomposites films in surface engineering, *J.Appl. Clay. Sci*., **135**, 75 (2017).
43. F. Lopresti, F. Carfì Pavia, I. Vitrano, M. Kersaudy-Kerhoas, V. Brucato, V. La Carrubba, Effect of hydroxyapatite concentration and size on morpho-mechanical properties of PLA-based randomly oriented and aligned electrospun nanofibrous mats, *J.Mech. Beh. Biomed. Mat*., **101**, 103449 (2020).
44. Q. Cai, Q. Xu,Q. Feng, X.Cao, X. Yang, X. Deng, Bio mineralization of electrospun poly(L-lactic acid)/gelatin composite fibrous scaffold by using a supersaturated simulated body fluid with continuous CO_2 bubbling, *J.Appl. Surf. Sci*., **257**, 10109 (2011).
45. S. Mallakpour, E. Khadem, Chitosan/$CaCO_3$-silane nanocomposites: synthesis, characterization, in vitro bioactivity and Cu(II) adsorption properties, *J. bio. Macromole.,* **114**, 149 (2018).
46. S. H. Lee, P.Md Tahir,W.C. Lum, L.P.Tan, P.Bawon, B.D.Park, U.H.Abdullah, A Review on Citric Acid as Green Modifying Agent and Binder for Wood, *J Poly* .,**12**, 1692 (2020).
47. N. A. A Zahrani, R. M. El-Shishtawy, A.M. Asiri, Recent developments of gallic acid derivatives and their hybrids in medicinal chemistry: A review, Eur *J .med chem*., 204, 112609 (2020)
48. V. R. Constantino, T. J. Pinnavaia, Basic properties of Mg^{2+} 1-x Al^{3+} x layered double hydroxides intercalated by carbonate, hydroxide, chloride, and sulfate anions, *J. Inorg. chem*., **34**, 883 (1995).
49. T. Kokubo, H. Takadama, How useful is SBF in predicting in vivo bone bioactivity? Biomaterials, *J. Biomat*., **27**, 2907 (2006).
50. M. Bukhtiyarova,. A review on effect of synthesis conditions on the formation of layered double hydroxides, *J.Sol. State. Chem.*, **269**, 494 (2019).
51. V. Trakoolwannachai, P.K heolamai, S. Ummartyotin, Characterization of hydroxyapatite from eggshell waste and polycaprolactone (PCL) composite for scaffold material, *J. Com. Part B: Eng*., **173,** 106974 (2019).